



CM-P00059201

CERN/EF/RF 82-1  
13 January 1982NEW RESULTS WITH SUPERCONDUCTING 500 MHz CAVITIES AT CERN

Ph. Bernard, G. Cavallari, E. Chiaveri, E. Haebel, H. Lengeler  
H. Padamsee<sup>(\*)</sup>, V. Picciarelli<sup>(\*\*)</sup>, D. Proch, A. Schwettman<sup>(\*\*\*)</sup>,  
J. Tückmantel and W. Weingarten<sup>(+)</sup>  
CERN, Geneva, Switzerland

H. Piel

University of Wuppertal, West Germany

ABSTRACT

New experimental results with three 500 MHz single cell Nb cavities of "spherical" shape are described. At 4.2 K acceleration fields up to 6.5 MV/m and  $Q_0$  values up to  $3 \times 10^9$  ( $1.7 \cdot 10^{10}$  at 2.2 K) have been reached. R.f. He ion sputtering was used and allowed to decrease electron loading sufficiently so that the fields were always limited by a thermal instability driven by a small region of increased r.f. losses. A stepwise removal of different lossy regions by mechanical grinding and milling allowed to increase field levels. It was found that the cavity performance depends strongly on the arrangement of the cavity and the vacuum system. After an accidental exposure to laboratory air no strong  $Q_0$  degradation was observed and the initial field value could be restored after a short He ion sputtering.

---

(\*) Scientific Associate from Cornell University, Ithaca, USA.

(\*\*) Scientific Associate from Bari University, Italy.

(\*\*\*) Scientific Associate from Stanford University, Palo Alto, USA.

(+) Fellow from University of Wuppertal, W. Germany.

## 1. INTRODUCTION

In 1979 a feasibility study for the application of sc acceleration cavities to LEP [1] was started at CERN. In a first series of measurements with a single cell [2] and a 4-cell Nb cavity [3], [4] at 500 MHz and of "spherical" shape very encouraging results were obtained. It was possible to reach in a single cell cavity with simple surface treatments at 4.2 K acceleration fields  $E_{acc}$  up to 4.1 MV/m and quality factors  $Q_0$  up to  $2.5 \times 10^9$ . In the 4-cell cavity  $E_{acc} = 2.8$  MV/m and  $Q_0 = 1.7 \cdot 10^9$  was obtained. Resonant electron loading (multipactor) was not observed.

The cavity performances were limited by dielectric losses, strong electron loading and by thermal instabilities due to point like lossy regions. In order to reach a better understanding of these limitations and in order to achieve a more comfortable margin of safety with respect to the design field of 3 MV/m more tests were performed and 2 cavities with a slightly modified geometry were constructed. One cavity was equipped with a coupling port for the fundamental high power coupler as needed for the operation in a storage ring; this necessitated a horizontal set up for the cold measurement. A marked difference of cavity behaviour in loss distribution and electron loading with respect to a vertical position was found. The excellent results obtained with He processing for decreasing electron loading in the 4-cell cavity had to be confirmed in a more systematic way. It also was attempted to increase field levels by a step wise removal of lossy regions by mechanical grinding and milling. A vacuum accident during which the cavity was exposed to laboratory air at atmospheric pressure lead us to try ways for restoring the cavity performance after an exposure to air. We note that similar studies with 500 MHz cavities are going in at KfK Karlsruhe [5] and KEK Japan [6].

## 2. THE CAVITIES

The cavity parameters have been computed by SUPERFISH [7], and some of them are given in table 1. The main dimensions are shown in fig. 1. For cavity II and III a different geometry and wall thickness from cavity I was chosen. The straight regions were made slightly conical in order to favour fast draining of liquids and in order to increase mechanical stiffness.

As we intend to construct a 5-cell structure of similar geometry for a test at PETRA/DESY the iris diameter was increased to 150 mm so that a coupling of  $\sim 1\%$  between cells is obtained. Cavities were fabricated by spinning and electron beam welding [2]. Cavity II was later on equipped with a coupling port for a high power fundamental coupler (fig. 1(b)). This port has an inner diameter of 76.9 mm. It is located at the equator and a hole had to be extruded at the cavity wall across the equatorial weld. Prior to this operation this weld had to be reinforced by a second welding from outside.

### 3. EXPERIMENTAL SET UPS AND PROCEDURES

#### 3.1 Experimental set up

The experimental set up used for cavity I in earlier experiments (test 3-15) has been described together with the diagnostic system in ref. [2]. It is shown in fig. 2(a). A major change with respect to this layout is the change to a horizontal position (i.e. a horizontal beam axis) during cold measurements (fig. 2(c)). This position implies no direct line of sight path between the cavity and warm parts of the vacuum system and reduces not only gas condensation but avoids also dust particles falling inside the cavity during mounting and operation. A similar layout was applied to cavity I from test 15 onwards (fig. 2(b)). The external magnetic field is slightly reduced by a magnetic shielding around the outer cryostat wall and amounts to  $\sim 100$  mG.

#### 3.2 Chemical treatments

The chemical treatment and inspection procedures applied to cavities prior to welding have been described in ref. [2]. After welding a chemical polish is normally applied. However, the first measurement of cavity II has been done after rinsing only. The final rinsing before a cold measurement is always performed with dust free distilled water in a vertical position. The cavity is dried in a laminar flow of dust free air while being in a horizontal position. All vacuum connections are performed under dust free conditions whenever possible.

### 3.3 R.f. and He ion sputtering

Already in previous experiments [2] it was found that r.f. processing can reduce the number and emissivity of electron sources. However, it was never possible to increase the field limit where electron loading sets in above 3.5 MV/m, a more typical value being 2.5 MV/m.

In order to overcome this low threshold He ion sputtering as proposed in ref. [8] has been applied. Because of the low frequency it should be particularly effective. We applied He ion sputtering in the following way. The ion sputtering pump is switched off and He gas of 99.997% purity is admitted with the help of a needle valve to a pressure of  $\sim 4 \cdot 10^{-5}$  mbar (measured at the warm part of the vacuum system) slightly below the gas discharge pressure. The r.f. field is increased at such a rate that no higher order modes are excited and/or no electron current larger than 30 pA is reached (as measured by an electron probe at the end of one beam tube (see fig. 2)).

### 3.4 Removal of lossy regions

Whenever electron loading could be overcome a fast quench due to a small region of increased r.f. losses was the ultimate field limit. As we don't know how to avoid safely these regions it is important to find a method for removing such defects. Temperature mapping supplies us with a possibility for localising such isolated regions and we followed a practice applied already at Argonne [9], Cornell [10] and Wuppertal [11] for treating such defects by mechanical grinding or by milling with a tungsten carbide tool. In these earlier experiments this procedure was always followed by a chemical polish. We know [2] that a chemical polish always produces a new surface with new defects and therefore we tried to do without a subsequent chemical polish. This is of considerable practical interest especially in large multicell cavities where a chemical polish would require large additional installations. The mechanical treatment is controlled by visual inspection and by a check of surface roughness. It is always followed by a degreasing and rinsing of the cavity.

#### 4. DISCUSSION OF RESULTS

In table 2 we give a summary of treatments, operating conditions and results of the three single cell cavities. In fig. 3 typical dependencies of  $Q_0$  values on field level are shown.

##### 4.1 Electron multipacting

The absence of any type of multipacting in the "spherical" geometry [2] has been once more confirmed for all experimental conditions and up to field levels of 7 MV/m. So far only cavities without coupling ports were measured. Only for such ideal cavities multipactor calculations can be performed and one has to check experimentally if openings in the cavity wall can cause multipacting. This was done with cavity II for a coupling port of the type foreseen for the high power input coupler in a 5-cell test cavity. Field levels up to 4.6 MV/m (cavity II, test 4 and 5) have been reached. No sign of multipactor was observed and the field was limited by a fast quench<sup>(\*)</sup>.

##### 4.2 R.f. Losses and their reduction

It has been shown previously [2] by our temperature mappings that one could distinguish different kinds of r.f. losses in the cavities.

- (a) BCS losses which are small in general as compared to other losses.
- (b) Homogeneous losses exceeding sometimes greatly the BCS losses. These losses were preferentially concentrated in the iris regions, dominated the measured  $Q$  values and showed strong "up-down" asymmetries (fig. 4(a)).
- (c) Point like defects with large r.f. losses which will give rise locally to high heat fluxes producing thermal instabilities.

---

(\*) The quench location is at the crossing of welds at the high power coupling port. There the magnetic field is enhanced by a factor of 1.5 compared to the undisturbed cavity.

#### 4.2.1 Homogeneous losses

Previous experiments had already shown that these losses can be made particularly small if the cavity is rinsed with dust free water and dried in a horizontal position. This was first shown in test No. 12 of cavity I and fig. 4(b) from ref. [2] shows the observed loss distribution. It only shows a very slight up-down asymmetry and the losses are partly caused by frozen in magnetic flux. This is confirmed by the test No. 2 of cavity III which was mounted in a horizontal position inside the cryostat. In fig. 4(c) the measured losses along the path of one resistor close to the equator are shown and compared to the computed distribution of the magnetic losses produced by an external magnetic field of  $\sim 100$  mG (see also fig. 5(b)).

Since the application of water rinsing and horizontal drying the achieved Q values have been systematically higher than in previous tests. The maximum  $Q_0$  achieved in test No. 14 of cavity I was  $1.7 \cdot 10^{10}$  at 2.2 K and corresponds to a residual resistance  $R_{res} = 15.6$  n Ohm. We attribute this Q improvement to the fact that the residues of the rinsing water are collected during the horizontal drying at the equator region i.e. in a region of high magnetic and vanishing electric field where dielectric losses are small.

#### 4.2.2 Lossy points and their removal

As in earlier tests, isolated points with much enhanced losses were found. After opening of the cavity they show up as dark spots sometimes with a halo as shown in fig. 6. Despite a careful investigation and an inspection with a specially designed scanning electron microscope [12] the nature of these dark spots remains unclear and we cannot yet decide whether they are due to material inclusions, to dust particles or to residues from the rinsing water. Sometimes scraping marks were found which were accidentally produced during previous surface inspections of the cavity. All isolated lossy regions show the previously observed  $E^2$ ,  $E^3$ ... dependence on field level and some switch reversibly at some definite field level to much higher r.f. losses [2].

Contrary to the previous experiments with cavity I non resonant electron loading (sect. 4.3) could be reduced to such an extent that in all relevant cases the field was limited by a thermal instability (quench) originating from a point like lossy region and discussed more in detail in ref. [2]. Quenches have been observed at different regions of the cavity where high magnetic and/or electric fields exist and at the weldings. They could always be related to a surface irregularity found by optical inspection or by a small scanning electron microscope which was introduced into the cavity [12]. Their surface resistance was found to be of the order of normal conducting material. The analysis of these quench regions and the process of thermal instability is continuing.

Lossy regions can show up as expected at the weldings (e.g. cavity III, run 1). It is nevertheless remarkable that there are so few of them and that the weld cannot be distinguished from its surroundings on the temperature maps up to the highest field levels achieved ( $E_{acc} = 7$  MV/m,  $H = 263$  G). A typical example for this is given in fig. 5(b).

It was a major goal to remove such lossy regions by a mechanical method followed by a cleaning procedure as described above. By sequentially treating and improving quench regions it was possible to increase the quench fields (see table 2)

for cavity I from 4.4 to 6 MV/m

for cavity II from 2.2 to 4.6 MV/m

for cavity III from 3.1 to 6.5 MV/m.

So far the most successful treatments [9,10,11] included as a last step a removal of a surface layer by chemical methods. Our aim is to avoid chemical polishing and to use other cleaning procedures which do not attack the Nb surface. In test 17-19 the field could be raised from 1.5 to 4.1 MV/m without chemical polish and by applying only a degreasing and rinsing. The field was no longer limited by a treated area but by a defect which became visible after achieving a

higher field level. The ground regions not treated by chemical polish are sometimes still visible on the temperature maps but their losses are greatly reduced although they had in one case a size of up to 10 cm<sup>2</sup>.

#### 4.3 Non resonant electron loading

We recall that non resonant electron loading produced by point like field emission electron sources situated in the region of  $E_p$  was the main field limitation in previous experiments [2]. Table 2 shows that electron loading remains a problem in cavities which are treated by chemical polish. (The threshold field where electron loading sets in is defined by the current at the electron probe  $i_e = 1$  pA). The exact nature of these electron sources is still unknown to us. Dust particles and condensed gases could be possible candidates. Therefore the experimental layout was modified in a way that during mounting and operation no dust from the vacuum system can fall into the cavity. This reduces in addition gas condensation due to cryo pumping from warm vacuum parts. After this a tendency towards lower electron loading was observed. This is illustrated e.g. by run No. 4 of cavity II where a quench field of 4.6 MV/m could be reached without electron loading. The point like nature, the low density, the preferential location of electron sources at the bottom of the cavity [2] and the reduction of their number in horizontally mounted cavities supports our opinion that dust particles are responsible for the electron emission observed in our cavities.

R.f. processing has been applied as in earlier experiments to reduce electron loading. However, it was never possible to increase the field limit where electron loading sets in above 3 MV/m. The field emission enhancement factors could be reduced to a range of 450-830.

He ion sputtering [8] has been applied systematically from test 14 onwards and proved to be in all cases a much more powerful method for decreasing electron loading. He processing can remove electron sources which resist to many hours of r.f. processing and the field levels up to which no electron loading is observed are in general much higher and range



up to 5.9 MV/m (in run 2 of cavity III). Correspondingly the  $\beta$  values are smaller and lie in the range of 340-600. He processing was found to be particularly effective after air exposures (run 17, run 19). The beneficial effects of He processing are preserved after a warm up to room temperature (test 18). He processing has allowed to decrease electron loading to a field level so that not only the quench field could be reached but that the  $Q_0$  value at the quench remains above  $10^9$ .

In no case has r.f. processing or He processing overcome a fast quench produced by point like defects of increased r.f. losses. This has been tested for processing periods up to  $\sim 24$  h.

#### 4.4 Accidental exposure to air

During an insertion of cavity No. 1 into its cryostat a vacuum accident occurred and the freshly prepared cavity was exposed within a few seconds to laboratory air at atmospheric pressure. By this accident dust contained in the air and dust from the vacuum system was deposited onto the cavity surface. As the handling of such an accident is of great practical importance for superconducting structures installed in an accelerator or storage ring we have tried to restore cavity performances. After repair, pump and cool down the cavity showed only a moderate  $Q$  degradation from  $2.4 \cdot 10^9$  in the preceding run to  $1.5 \cdot 10^9$ . The most obvious effect was a strong increase in electron loading which started already at 0.3 MV/m. After 1 h r.f. processing no decrease was observed and therefore a He ion sputtering was applied. After 3 h a field of 4 MV/m with  $Q_0 = 1.2 \cdot 10^9$  was reached which was limited by a quench. In order to check the beneficial effect of He processing the cavity was warmed up to room temperature and cooled down again. No change in cavity performances was observed. The influence of dust during an exposure to laboratory air was checked in the next experiments. The cavity was exposed at room temperature slowly ( $\sim 1.5$  h) to air and remained at atmospheric pressure for three days. A dust filter was used and it is expected that the slow exposure to air did not transport dust particles from the vacuum system to the cavity. No degradation in  $Q_0$  was observed and the field could be raised to its initial value after 1 h of r.f. processing. A third test was

performed in order to investigate the role of dust from the vacuum system. The cavity was kept at 4.2 K and was exposed by a sudden opening of a valve and without dust filter to  $\sim 300$   $\mu$  of He gas (purity 99.997%). No  $Q_0$  degradation at low field was observed; Electron loading was produced but could be overcome by He ion sputtering and the initial field value was reached again. The two last tests performed after the cavity had been exposed to a field of 4 MV/m do confirm results in air exposure at KfK Karlsruhe [13] but do not confirm the  $Q_0$  degradation observed recently at KEK, Japan [6].

#### Acknowledgements

We thank all technicians and engineers of our group for their help. This work had to rely strongly on the skill and competence of the SB workshops for spinning, electron beam welding and chemical treatments. We also thank the EF workshop and cryogenic group for their help. The support of the vacuum group of ISR Division and of SB Division in the surface investigations is gratefully acknowledged.

REFERENCES

- [1] CERN/ISR-LEP/79-33 (1979).
- [2] Ph. Bernard, G. Cavallari, E. Chiaveri, E. Haebel, H. Heinrichs, H. Lengeler, E. Picasso, V. Picciarelli, J. Tückmantel and H. Piel, Nucl. Instr. Meth. 190 (1981) 257.
- [3] Ph. Bernard et al., CERN/EF/RF 81-2.
- [4] Ph. Bernard et al., CERN/EF/RF 81-7.
- [5] Sh. Noguchi, Y. Kojima and J. Halbritter, Nucl. Instr. Meth 179 (1981) 205.
- [6] Y. Kojima, T. Furuga and T. Nakazato to be publ. in Japan Journal App. Phys.
- [7] K. Halbach and R.F. Holsinger, Part. Acc. 7 (1976) 213.
- [8] H.A. Schwettman, J.P. Turneaure and R.F. Waites, Journal Appl. Phys. 45 (1974) p. 914.
- [9] K.W. Shepard, C.H. Scheibelhut, P. Markovich, R. Benaroya and L.M. Bollinger, IEEE Trans. Mag. MAG-15 666 (1979).
- [10] H. Padamsee et al., IEEE Mag. 13 (1977) 346.
- [11] U. Klein, D. Proch and T. Grundey, IEEE Trans-NS-28 (1981) 3222.
- [12] A.G. Mathewson and A. Grillot, CERN Inter. Note CERN-ISA-VA/81-34.
- [13] W. Bauer, private communication.

TABLE 1

Some parameters<sup>(a)</sup> of the 500 MHz single cell cavities

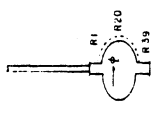
	Cavity I	Cavity II and III
Frequency (MHz)	494.7	~ 501
Quality factor Q (Cu at 300 K)	45852	46869
$\frac{\text{Shunt impedance}}{\text{quality factor}} \frac{\text{Ohm}}{\text{m}}$	533	451
$E_p/E_{\text{acc}}^{(b)}$	2.00	1.94
$H_p/E_{\text{acc}} \frac{0e}{(\text{MV/m})}$	34.2	37.6
Geometry factor (Ohm)	266.1	272
$\Delta f/\Delta p^{(c)}$ (Hz/mbar)	250	74 (without coupling port) 160 (with coupling port)

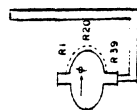
(a) Computed by SUPERFISH

(b)  $E_{\text{acc}} = 2/\lambda \cdot \int_0^l E_z e^{ikz} dz$  with  $l$ : total length of cavity including beam tubes

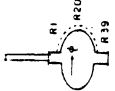
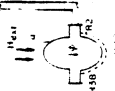
(c) Measured at 4.2 K - 2.2 K

Cavity No. I

Experimental layout	Test No.	Treatments operation conditions	Low field $Q_{4,2K}$ $\times 10^9$	$\beta$	Eacc without $e^-$ maximum 4,2 K, CW	Field limitation	Comments	
	13	Bake out 200°C, leak at cool down	2.0 (5.0)	510	2.6	4.4	Magnetic shielding light emission	
	14	CP (18 $\mu$ m)	> 2.6 (17)	-	2.0	-	quench at R30	lossy regions R30, R14, 1224
		3 1/2 h He processing	-	570	3.0	2.8	quench at R14	scraping marks at R14
	15	Scraping and milling R30, R14	1.9 (3,8)	1370	1.5	1.8	quench at R11	scratch at R11 carbonised rag in pumping line
		no CP	2.4 (7.1)	-	-	1.5	e <sup>-</sup> loading	many e <sup>-</sup> trajectories
	16	Milling R14, no CP	1.5 (2.3)	7200	0.3	0.6	e <sup>-</sup> loading	scratch at R9
		Milling R11, R14, no CP	1.5	-	0.3	0.6	e <sup>-</sup> loading	quench at R9
		Vacuum accident at 300 K	1.7 (3.9)	590	2.6	4.0	quench at R9	quench at R9
	17	1 h r.f. processing	1.7 (3.9)	3000	0.5	-	-	-
		3h He processing	1.7	9000	2.6	4.0	quench at R9	quench at R9
		Warm up to 300 K	1.8	600	1.1	3.4	e <sup>-</sup> loading	quench at 4 MV/m
		1h r.f. processing	-	830	2.1	3.4	e <sup>-</sup> loading	quench at R9
		Fast exposure to He gas at 4,2 K	1.8	600	2.5	4.1	quench at R9	quench at R9
18	1h r.f. processing	2.2	-	2.5	-	no attempt to reach quench	-	
	3h He processing	2.2 (6.1)	410	4.6	6.0	quench at equator region	quench at equator region	
19	Milling R9, CP (30 $\mu$ m)	2.2	-	2.5	-	no attempt to reach quench	-	
	2h of He processing	2.2 (6.1)	410	4.6	6.0	quench at equator region	quench at equator region	
20	1h r.f. processing	2.2	-	2.5	-	no attempt to reach quench	-	
	3h He processing	2.2 (6.1)	410	4.6	6.0	quench at equator region	quench at equator region	



Cavity No. II

Experimental layout	Test No.	Treatments Operation conditions	Low field $Q_e$ 4,2K (2.2K) $\times 10^9$	$\beta$	Eacc (MV/m) without $e^-$	Field limitation	Comments
	1	Milling of half cells no CP after welding He processing 2 days	1.1 -	1500 820	1.5 1.5	1.0 -	not tried to reach quench no magnetic shielding
	2	Welding of coupler tube CP (18 $\mu$ m)	1.65	-	2.2	quench at crossing of welds	Welding beads
	3	Milling at equatorial weld near coupling tube no CP	1.5	-	2.2	quench at crossing of welds	
	4	Milling of equatorial and circular weld of coupling tube CP (36 $\mu$ m)	1.74	-	4.6	quench at weld	
	5	Only warm up to 300 K	1.77 (3.3)	-	4.6	quench at weld	

Cavity No. III

Test No.	Treatments	3	-	> 3.07	3.07	quench at weld	Magnetic shielding to 100 mG
1	Milling and grinding of weldings CP (18 $\mu$ m)	3 (11)	-	> 3.07	3.07	quench at weld	Magnetic shielding to 100 mG
2	Grinding of quench region CP (18 $\mu$ m)	3 (> 16)	720	3.2	5.02	slow breakdown	
	r.f. processing	3	430	4.2	6.5	quench at R24	2 $e^-$ trajectories
	2 x 12 h He processing	3	340	5.9	6.5	"	electron trajectories disappeared

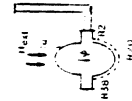


FIGURE CAPTIONS

Fig. 1 Main dimensions and weldings of the single cell cavities;  
weldings are indicated by "W"

(a) Cavity I

(b) Cavity II and III

Cavity III is not equipped with a coupling port.

Fig. 2 Experimental layouts

A: fixed r.f. input coupler

B: r.f. probe

C: electron probe

D: pumping line

E: dust filter

F: coupling port (cavity II)

G: cryostat cover

R1-R39 movable resistors for temperature mapping.

Fig. 3 Measured dependence of Q values on  $E_{acc}$  for different cavities  
and working conditions. Field enhancement factors  $\beta$  are  
indicated. For the run numbers see Table 2.

Fig. 4 (a) Mean power density due to r.f. losses for 39 resistors after  
a chemical polish and a drying in vertical position (run 2 of  
ref. [2]). The corresponding  $H^2$  and  $E^2$  distributions are  
given in fig. 4(b).  $\bar{p}'$  is obtained by integration of r.f. losses  
for  $0^\circ \leq \varphi \leq 360^\circ$ .

FIGURE CAPTIONS (Cont'd)

(b) Same as (a) after a chemical polish and a drying in horizontal position (run 12 of ref. [2]). For comparison the curves for  $E^2$ ,  $H_{r.f.}^2$  and for  $H_{ext} \cos \alpha H_{r.f.}^2$  are given. For the direction of  $H_{ext}$  and for  $\alpha$  see insert;  $H_{r.f.}$  is the r.f. magnetic field at the resistor positions.

(c) Power density due to r.f. losses at resistor R18 for run 2 of cavity III which was measured in a horizontal position. The points are fitted with the curve  $H_{ext} \cdot \cos \varphi$ ; for  $\varphi$  and the direction of  $H_{ext}$  see insert.

Fig. 5 Temperature maps of cavity III, run 2; for the layout of movable resistors see fig. 2. (a) Prior to He processing, two electron trajectories can be seen,  $E_{acc} = 6.7$  MV/m. (b) After He processing, the electron trajectories are no longer visible;  $E_{acc} = 7$  MV/m ( $T_b = 2.7$  K,  $Q_0 = 1.6 \cdot 10^{10}$ ).

Fig. 6 (a) Photography of a quench region (test 14, R30), the diameter of the halo is  $\sim 1.5$  mm.

(b) Same region as seen by a small scanning electron microscope installed inside the cavity. A few insulating regions are distinguishable but the nature of this region is unknown.





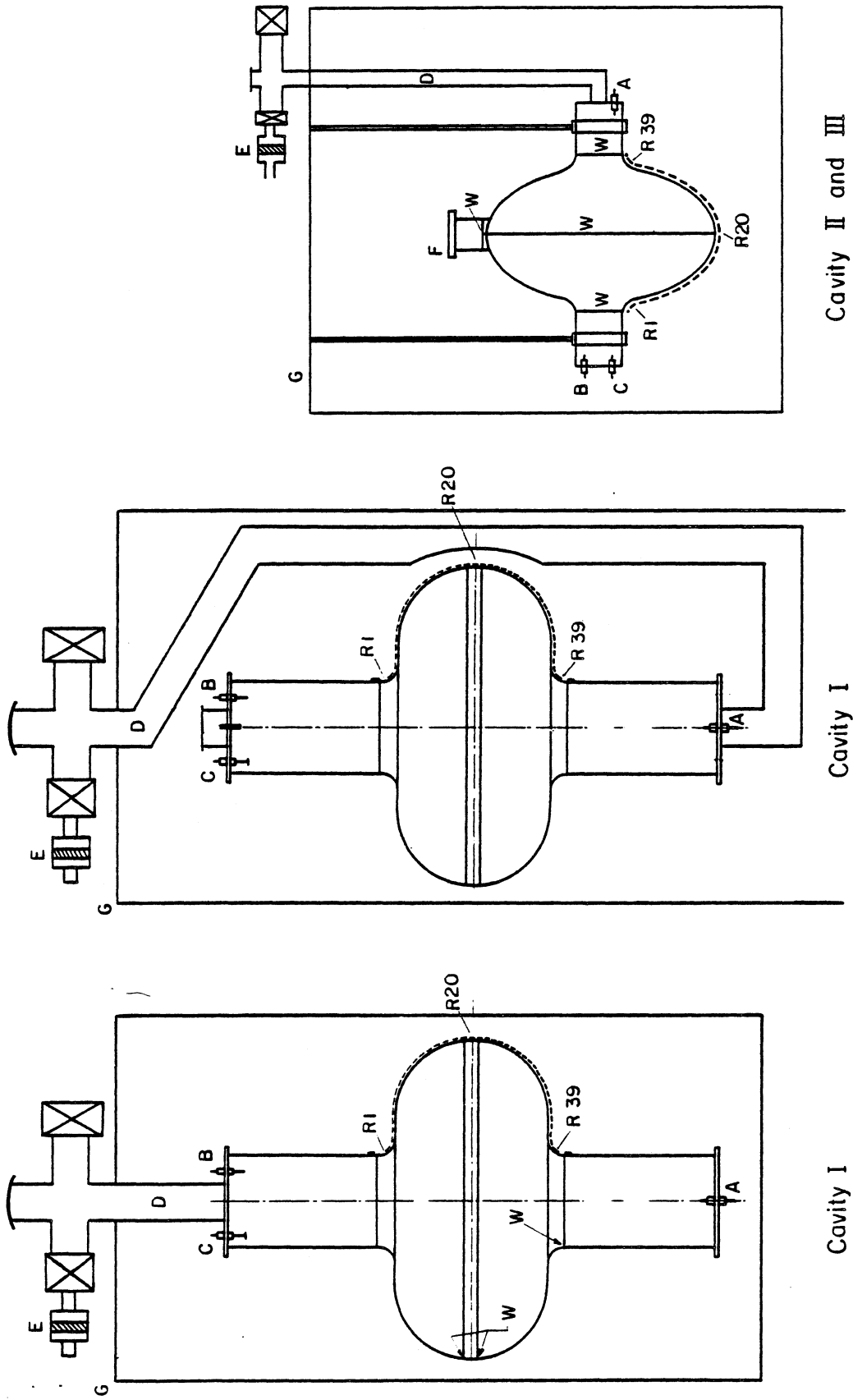


Fig. 2

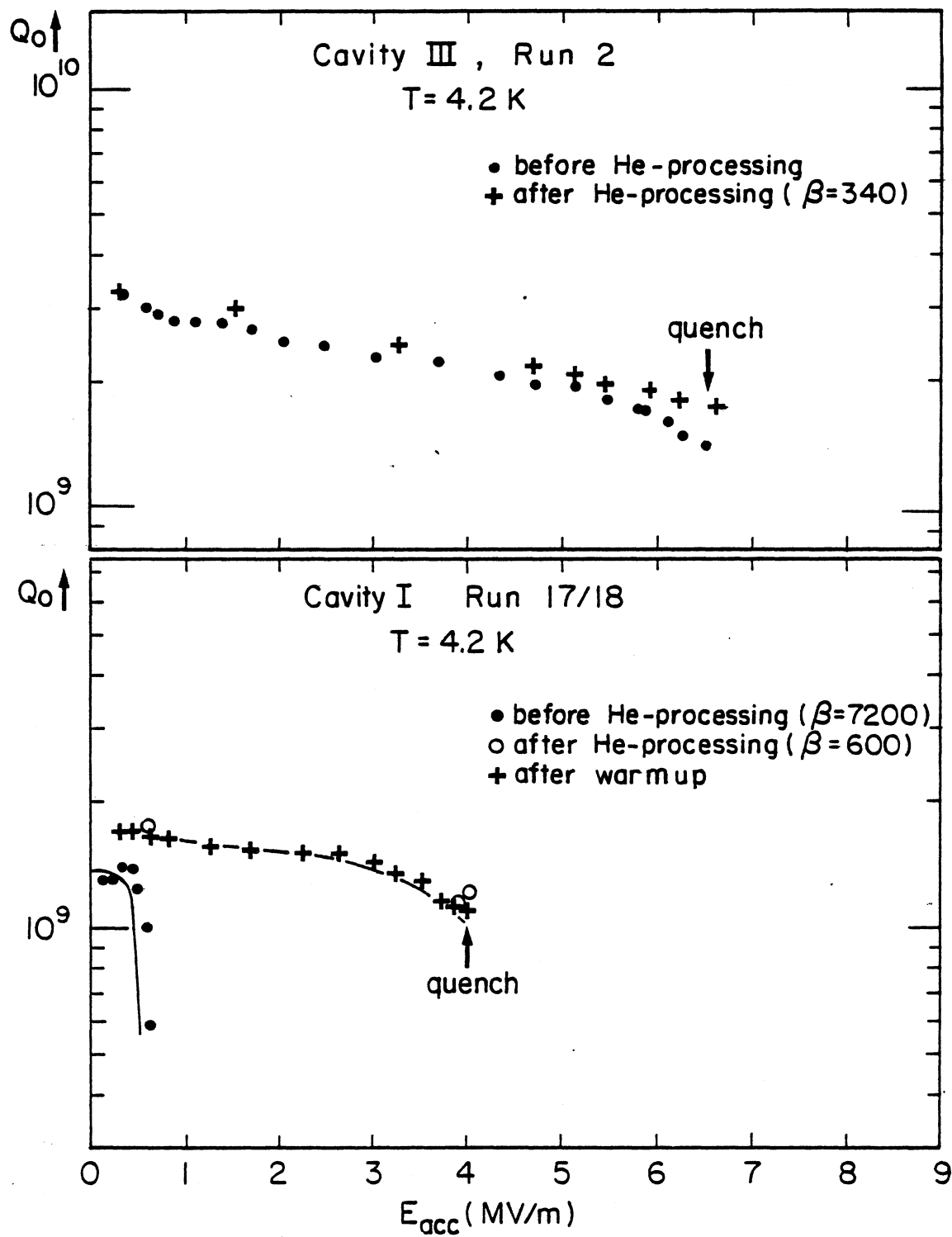


Fig. 3

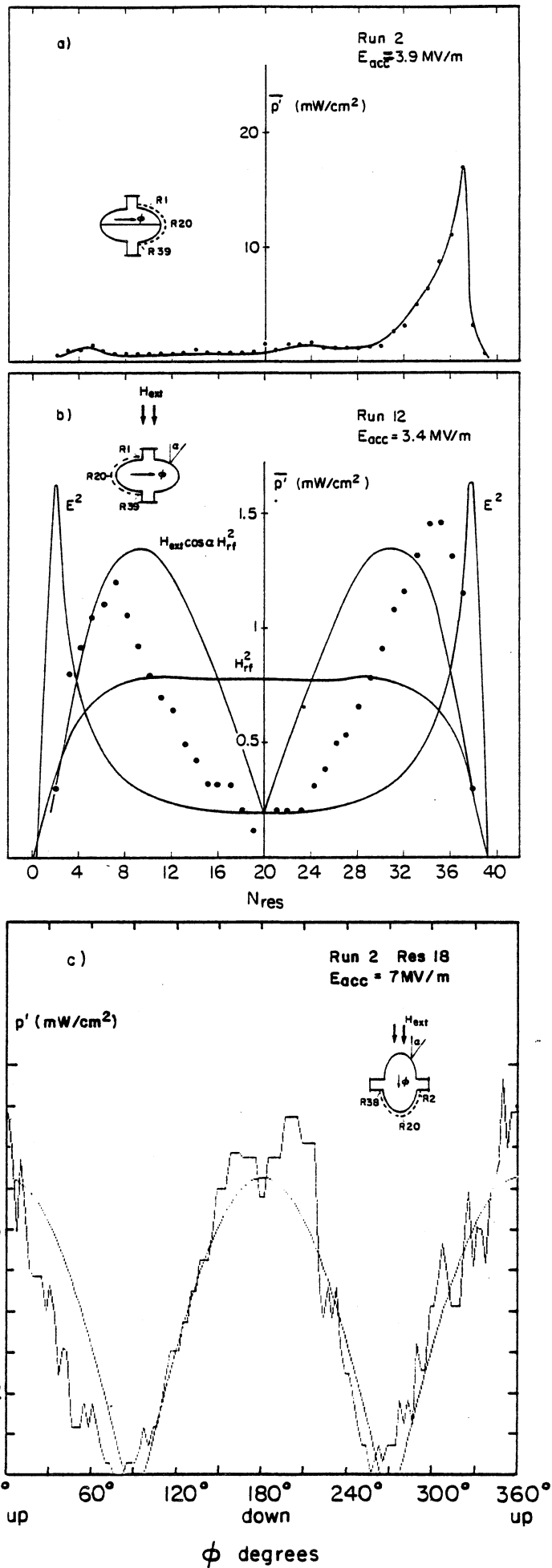


Fig. 4

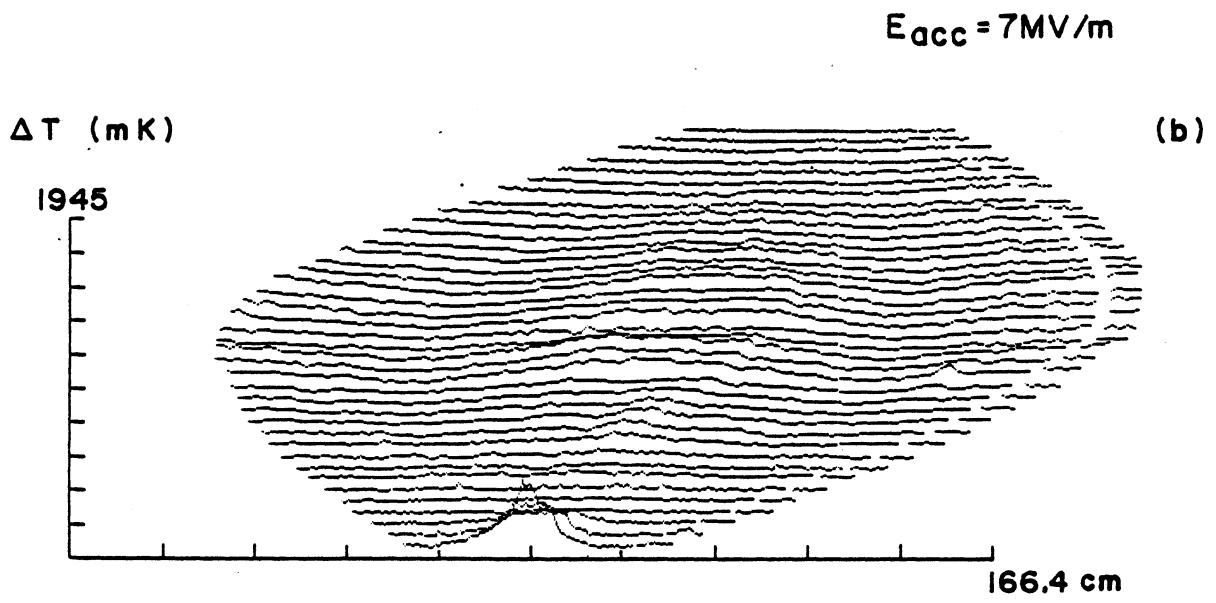
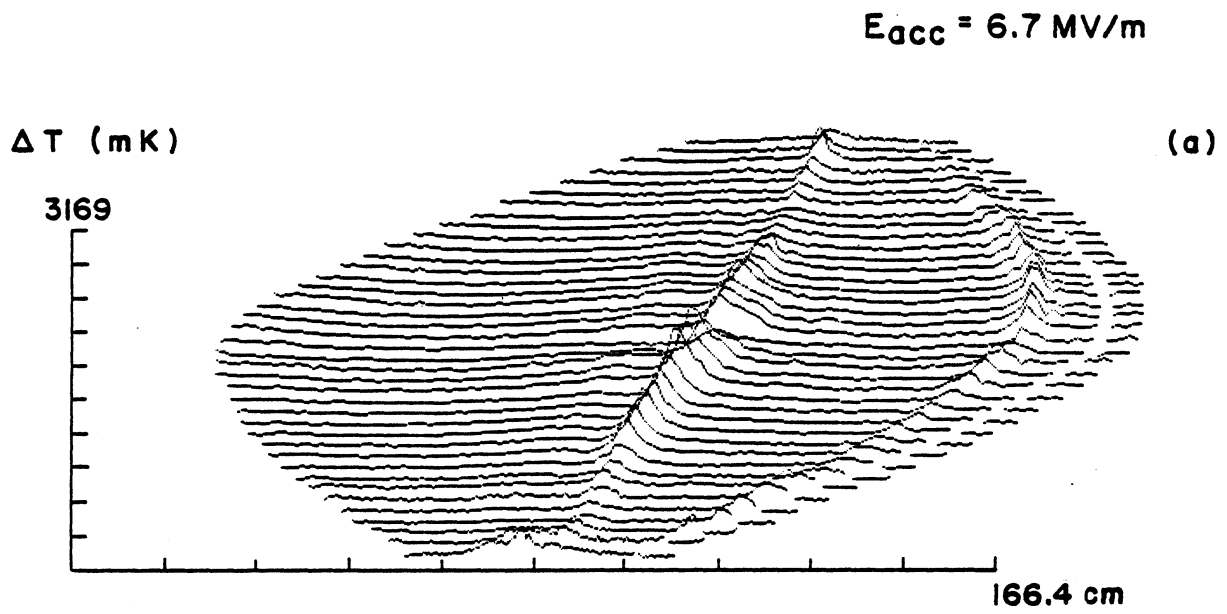
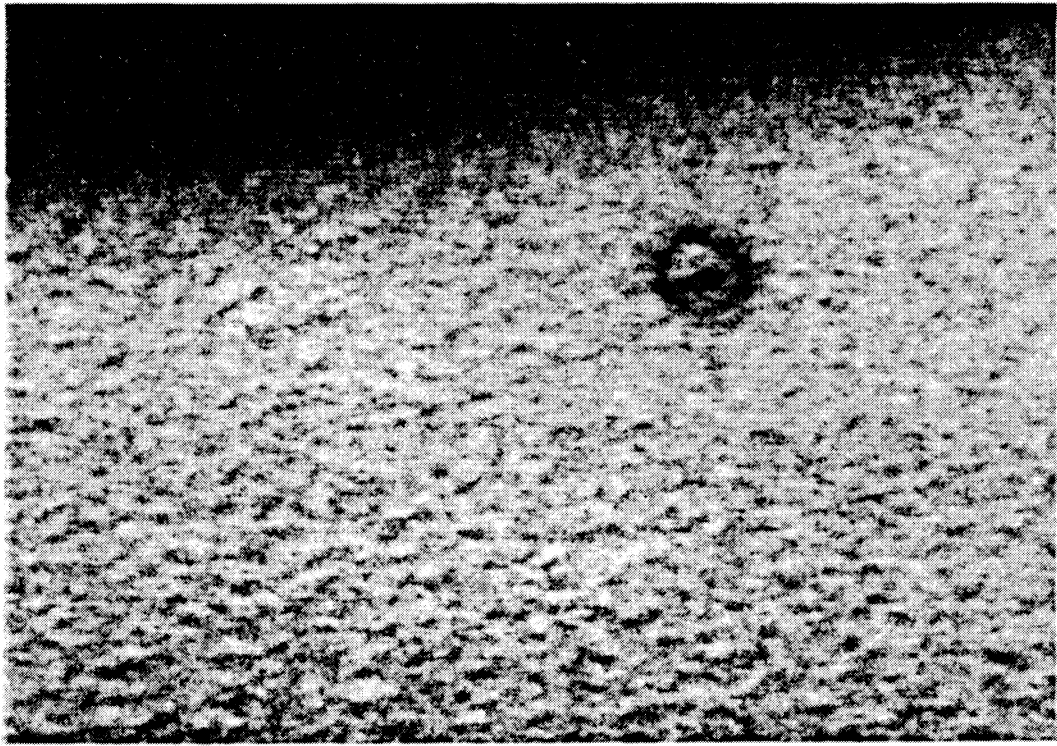


Fig. 5

a)



b)

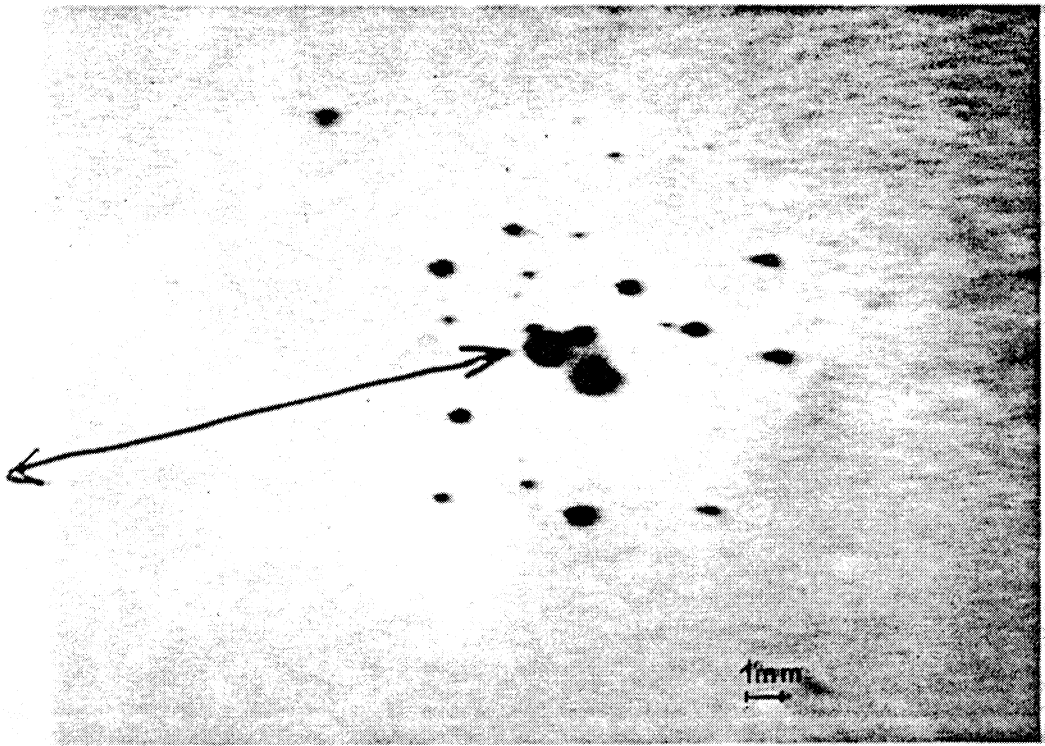


Fig. 6